19th International Conference
ENGINEERING MECHANICS 2013
Svratka, Czech Republic, May 13 – 16, 2013

# Distance-based and stress-based gradient-enhanced damage models

**M. Horák** [1] **, M. Jirásek** [2]

**Summary:** *Damage mechanics is a suitable framework for description of the behavior of quasibrittle materials. However, the classical theory fails after the loss of ellipticity of the governing differential equation. From the numerical point of view, loss of ellipticity is manifested by a pathological dependence of the results on the size and orientation of finite elements. To avoid such an undesired behavior, the model can be regularized by an implicit gradient formulation. However, this enhancement in its usual form leads to excessive energy dissipation near non-convex boundaries (e.g. notches and obtuse corners). This paper describes two modifications of the standard gradient-enhanced damage formulation and their implementation into a finite element code. The difference between the formulations is illustrated by a numerical example.*

## 1. Introduction

Realistic description of the mechanical behavior of quasibrittle materials such as concrete requires constitutive laws with softening. From the physical point of view, softening can be attributed to the propagation and coalescence of defects, e.g. voids and cracks. It is well known that softening may lead to localization of inelastic strain into narrow process zones. For traditional models formulated within the classical framework of continuum mechanics, such zones have an arbitrarily small thickness, and failure can occur at extremely low energy dissipation, which is not realistic. The mathematical model becomes ill-posed and the numerical solutions suffer by pathological sensitivity to the discretization parameter, e.g. to the size of finite elements. It is therefore necessary to introduce special enhancements acting as localization limiters.

This paper deals with the implicit gradient enhancement. Within this framework, the mathematical model remains well-posed and numerical results are mesh objective. However, the standard implicit gradient enhancement may result in excessive energy dissipation near non-convex boundaries, and its modifications are necessary to reduce this spurious effect (Bažant et al., 2010; Giry et al., 2011).

The paper is organised as follows. In Section 2 the classical isotropic damage mechanics is outlined. In Section 3 the implicit gradient-enhanced formulation is described and its distance-based and stress-based modifications to reduce spurious dissipation near boundaries

[1] Ing. Martin Horák, Department of Mechanics, Faculty of Civil Engineering, Czech Technical University in Prague, Thákurova 7, 166 27, Prague; CZ, e-mail: martin.horak@fsv.cvut.cz
[2] Prof. Ing. Milan Jirásek, DrSc., Department of Mechanics, Faculty of Civil Engineering, Czech Technical University in Prague, Thákurova 7, 166 27, Prague; CZ, e-mail: milan.jirasek@fsv.cvut.cz

are introduced. The links to the micromorphic formulation are discussed. In Section 4, implementation of the regularized damage model into a finite element code is described. Finally, the performance of the modified regularized models is assessed by simulations of a three-point bending test of concrete specimens with a sharp notch and a V-shaped notch.

## 2. Damage mechanics

In this section, we consider a family of simple isotropic damage models with one scalar damage variable $\omega$, driven by the equivalent strain. The basic equations consist of the stress-strain law

$$\boldsymbol{\sigma} = (1-\omega)\,\bar{\boldsymbol{\sigma}} = (1-\omega)\,\boldsymbol{D}_e : \boldsymbol{\varepsilon} \tag{1}$$

damage law

$$\omega = g(\kappa) \tag{2}$$

and loading-unloading conditions

$$f(\boldsymbol{\varepsilon},\kappa) \leq 0 \qquad \dot{\kappa} \geq 0 \qquad \dot{\kappa} f(\boldsymbol{\varepsilon},\kappa) = 0 \tag{3}$$

with the damage loading function $f$ defined as

$$f(\boldsymbol{\varepsilon},\kappa) = \tilde{\varepsilon}(\boldsymbol{\varepsilon}) - \kappa \tag{4}$$

In the above equations, $\boldsymbol{\sigma}$ is the stress tensor, $\bar{\boldsymbol{\sigma}}$ is the effective stress tensor, $\omega$ is a scalar damage variable, $\boldsymbol{D}_e$ is the elastic stiffness tensor, $\boldsymbol{\varepsilon}$ is the small-strain tensor, $g$ is the damage evolution function, $\tilde{\varepsilon}$ is a scalar measure of the strain level called the equivalent strain, and $\kappa$ is an internal variable which corresponds to the maximum level of equivalent strain ever reached in the previous history of the material. The choice of the specific expression for the equivalent strain directly affects the shape of the elastic domain in the strain space (and, as a consequence, also in the stress space).

## 3. Implicit gradient regularization

In the previous section, a simple local damage model has been introduced. Here we focus on its regularization by the implicit gradient formulation. Equations (2)–(4) are reformulated using the nonlocal equivalent strain $\bar{\varepsilon}$ and the corresponding history variable $\bar{\kappa}$, which represents the maximum level of the nonlocal equivalent strain. The equations are rewritten as

$$\omega = g(\bar{\kappa}) \tag{5}$$

$$f(\bar{\varepsilon},\bar{\kappa}) \leq 0 \qquad \dot{\bar{\kappa}} \geq 0 \qquad \dot{\bar{\kappa}} f(\bar{\varepsilon},\bar{\kappa}) = 0 \tag{6}$$

$$f(\bar{\varepsilon},\bar{\kappa}) = \bar{\varepsilon} - \bar{\kappa} \tag{7}$$

In the standard gradient-enhanced model, the nonlocal variable $\bar{\varepsilon}$ is computed from a Helmholtz-like differential equation

$$\bar{\varepsilon} - l^2 \nabla^2 \bar{\varepsilon} = \tilde{\varepsilon} \tag{8}$$

with the homogeneous Neumann boundary condition

$$\boldsymbol{n} \cdot \boldsymbol{\nabla} \bar{\varepsilon} = 0 \tag{9}$$

applied on the entire boundary $S$ of the spatial domain $V$ occupied by the body of interest. In the equations above, $l$ is the characteristic length (related to the size and spacing of major heterogeneities in the material microstructure), $\tilde{\varepsilon}$ is the local equivalent strain computed directly from the strain tensor $\boldsymbol{\varepsilon}$, $\boldsymbol{\nabla}$ is the gradient operator, $\nabla^2 = \boldsymbol{\nabla} \cdot \boldsymbol{\nabla}$ is the Laplace operator, and $\boldsymbol{n}$ is the outward unit normal to the boundary.

The implicit gradient formulation acts as a proper regularization technique and overcomes problems with fracture at extremely low dissipation caused by localization of damage to a single layer of finite elements; however, in its standard form it leads to excessive energy dissipation close to non-convex boundaries. This problem may be alleviated by a suitable modification. Here we consider a generalized version of equation (8), which permits more flexibility and can emphasize the influence of the distribution of the local field $\tilde{\varepsilon}$ in certain directions. For this purpose, the scalar characteristic length $l$ is replaced by a second-order tensor $\boldsymbol{L}$, and (8) is generalized to

$$\bar{\varepsilon} - \nabla \cdot \left( \boldsymbol{L}^2 \cdot \nabla \bar{\varepsilon} \right) = \tilde{\varepsilon} \tag{10}$$

### 3.1. Distance-based and stress-based modifications

Two modifications considered here are inspired by the work of Xenos et al. (2013) who dealt with an integral nonlocal formulation (in contrast to the present implicit gradient formulation) and constructed special weight functions for nonlocal averaging, in the spirit of Bažant et al. (2010) and Giry et al. (2011). Here we reformulate this idea in the implicit gradient setting.

First we consider the so-called **distance-based modification**. In this formulation, the scalar internal length parameter $l$ is considered as variable in space and is adjusted near boundaries by a dimensionless reduction factor

$$\gamma_d = \begin{cases} 1, & \text{if } \; d(\boldsymbol{x}) \geq t l_0 \\ \\ \beta + \dfrac{1-\beta}{t l_0} d(\boldsymbol{x}), & \text{if } \; d(\boldsymbol{x}) < t l_0 \end{cases} \tag{11}$$

where $t$ and $\beta$ are dimensionless model parameters and $d(\boldsymbol{x})$ denotes the distance of point $\boldsymbol{x}$ from the specimen boundary. The position-dependent characteristic length is then

$$l = \gamma_d l_0 \tag{12}$$

where $l_0$ is a constant that corresponds to the characteristic length far from the boundaries.

In the **stress-based approach**, the orientation and intensity of nonlocal interactions are modified according to the stress state. The second-order internal length tensor $\boldsymbol{L}$ is introduced. Under plane stress, it can be represented by the spectral decomposition

$$\boldsymbol{L} = l_1 \boldsymbol{n}_1 \otimes \boldsymbol{n}_1 + l_2 \boldsymbol{n}_2 \otimes \boldsymbol{n}_2 \tag{13}$$

where $\boldsymbol{n}_1$ and $\boldsymbol{n}_2$ are the unit eigenvectors of the stress tensor associated with the larger and smaller principal stresses, respectively, $l_1 = l_0$ is constant, and $l_2 = \gamma_s l_0$ with

$$\gamma_s = \begin{cases} 1 & \text{if } \hat{\sigma}_1 \leq 0 \\ \\ \left( \beta + (1-\beta) \dfrac{\langle \hat{\sigma}_2 \rangle^2}{\hat{\sigma}_1^2} \right) & \text{if } \hat{\sigma}_1 > 0 \end{cases} \tag{14}$$

The principal stresses $\hat{\sigma}_1$ and $\hat{\sigma}_2$ (eigenvalues of the stress tensor) are ordered such that $\hat{\sigma}_1 \geq \hat{\sigma}_2$. They are equal to the principal effective stresses $\bar{\sigma}_1$ and $\bar{\sigma}_2$ multiplied by the same factor $1-\omega$, and so it is possible to replace in (14) $\hat{\sigma}_1$ by $\bar{\sigma}_1$ and $\hat{\sigma}_2$ by $\bar{\sigma}_2$. The advantage is that the principal effective stresses can be directly computed from the strains, without knowing the value of the damage variable $\omega$. In (14), $\beta$ is a dimensionless model parameter and $\langle\cdot\rangle$ are MacAuley brackets (denoting the positive part).

### 3.2. Micromorphic formulation

The implicit gradient damage formulation lacks a solid thermodynamic basis. For this reason we demonstrate the similarity of the implicit gradient formulation to the thermodynamically consistent micromorphic approach; see Forest (2009) for a general overview. We start from the principle of virtual power

$$P^{int} = P^{ext} \tag{15}$$

where $P^{int}$ is the (extended) virtual power of internal forces and $P^{ext}$ is the virtual power of external forces. The virtual power of internal forces is extended by terms that represent the contribution of the so-called micromorphic variable (here the nonlocal equivalent strain) and its gradient. Therefore, the density of internal virtual power is defined as

$$p^{int} = \boldsymbol{\sigma} : \dot{\boldsymbol{\varepsilon}}^* + s\dot{\bar{\varepsilon}}^* + \boldsymbol{s} : \boldsymbol{\nabla}\dot{\bar{\varepsilon}}^* \tag{16}$$

where $\dot{\boldsymbol{\varepsilon}}^*$ is the virtual strain rate, $\dot{\bar{\varepsilon}}^*$ is the virtual equivalent strain rate, and $s$ and $\boldsymbol{s}$ are generalized stresses conjugated to the micromorphic variable $\bar{\varepsilon}$ and its gradient $\boldsymbol{\nabla}\bar{\varepsilon}$. Integrating the power density (16), we obtain the internal virtual power

$$P^{int} = \int_V p^{int}\mathrm{d}V \tag{17}$$

In general, the virtual power of external forces could also be enhanced by terms that correspond to generalized body forces and generalized tractions, but in the present context it is sufficient to use the standard expression

$$P^{ext} = \int_{S_t} \boldsymbol{t} \cdot \dot{\boldsymbol{u}}^* \mathrm{d}S \tag{18}$$

where $\boldsymbol{t}$ are the prescribed tractions on the boundary, $\dot{\boldsymbol{u}}^*$ is the virtual displacement rate, and the (standard) body forces are considered as negligible. $S_t$ is the free (unsupported) part of the boundary. On the supported part of the boundary, $S_u$, the virtual displacement rate $\dot{\boldsymbol{u}}^*$ vanishes and thus the unknown reactions do not contribute to the virtual power in (18).

The virtual work equality (15) combined with the kinematic equations and kinematic boundary conditions leads to the standard and generalized equilibrium equations

$$\nabla \cdot \boldsymbol{\sigma} = \boldsymbol{0} \qquad \text{in} \quad V \tag{19}$$

$$\nabla \cdot \boldsymbol{s} = s \qquad \text{in} \quad V \tag{20}$$

and boundary conditions

$$\boldsymbol{\sigma} \cdot \boldsymbol{n} = \boldsymbol{t} \qquad \text{on} \quad S_t \tag{21}$$

$$\boldsymbol{s} \cdot \boldsymbol{n} = 0 \qquad \text{on} \quad S \tag{22}$$

To get the state laws governing the generalized stresses, we introduce the Helmholtz free energy density enhanced by additional micromorphic terms,

$$\Psi = \tfrac{1}{2}(1-\omega)\boldsymbol{\varepsilon} : \boldsymbol{D}_e : \boldsymbol{\varepsilon} + \tfrac{1}{2}A\left(\tilde{\varepsilon} - \bar{\varepsilon}\right)^2 + \nabla\bar{\varepsilon} \cdot \boldsymbol{C} \cdot \nabla\bar{\varepsilon} \tag{23}$$

with a new scalar parameter $A$ and second-order tensorial parameter $\boldsymbol{C}$. The dissipation inequality (for isothermal processes)

$$D = p^{int} - \dot{\Psi} \geq 0 \tag{24}$$

combined with (16) and (23) then yields

$$D = \left(\boldsymbol{\sigma} - \frac{\partial\Psi}{\partial\boldsymbol{\varepsilon}}\right) : \dot{\boldsymbol{\varepsilon}} + \left(s - \frac{\partial\Psi}{\partial\bar{\varepsilon}}\right)\dot{\bar{\varepsilon}} + \left(\boldsymbol{s} - \frac{\partial\Psi}{\partial\nabla\bar{\varepsilon}}\right) \cdot \dot{\boldsymbol{\varepsilon}} - \frac{\partial\Psi}{\partial\omega}\dot{\omega} \geq 0 \tag{25}$$

Assuming that the terms related to micromorphic variables are non-dissipative, we get the state laws

$$s = \frac{\partial\Psi}{\partial\bar{\varepsilon}} = -A(\tilde{\varepsilon} - \bar{\varepsilon}) \tag{26}$$

$$\boldsymbol{s} = \frac{\partial\Psi}{\partial\nabla\bar{\varepsilon}} = \boldsymbol{C} \cdot \nabla\bar{\varepsilon} \tag{27}$$

$$\boldsymbol{\sigma} = \frac{\partial\Psi}{\partial\boldsymbol{\varepsilon}} = (1-\omega)\boldsymbol{D}_e : \boldsymbol{\varepsilon} + A\left(\tilde{\varepsilon} - \bar{\varepsilon}\right)\frac{\partial\tilde{\varepsilon}}{\partial\boldsymbol{\varepsilon}} \tag{28}$$

and the reduced dissipation inequality

$$-\frac{\partial\Psi}{\partial\omega}\dot{\omega} = \frac{\dot{\omega}}{2}\boldsymbol{\varepsilon} : \boldsymbol{D}_e : \boldsymbol{\varepsilon} \geq 0 \tag{29}$$

Since the stiffness tensor is positive definite and damage can only grow, condition (29) is always satisfied and the model is consistent with the second law of thermodynamics.

Substituting (26)–(27) into (20) and taking into account that $A$ is a constant, we arrive at

$$\bar{\varepsilon} - \nabla \cdot \left(\frac{1}{A}\boldsymbol{C} \cdot \nabla\bar{\varepsilon}\right) = \tilde{\varepsilon} \tag{30}$$

This corresponds to the implicit gradient equation in its generalized form (10) with $\boldsymbol{L}^2 = \boldsymbol{C}/A$. If tensor $\boldsymbol{L}$ is constant in time and depends only on the spatial variable, the equivalence is perfect. However, for the stress-based formulation $\boldsymbol{L}$ changes in time depending on the evolution of stress, which is not considered by the micromorphic model.

Substituting (27) into (22), we get the boundary condition

$$(\boldsymbol{C} \cdot \nabla\bar{\varepsilon}) \cdot \boldsymbol{n} = 0 \tag{31}$$

For the standard implicit gradient model as well as for its distance-based modification, $\boldsymbol{C}$ is a multiple of the unit second-order tensor and condition (31) is equivalent to the homogeneous Neumann boundary condition (9). For a general tensor $\boldsymbol{C}$, these conditions would differ.

In summary, the boundary value problem defining the nonlocal variable according to the standard and distance-based implicit gradient formulations can be derived from the micromorphic formulation using a thermodynamically consistent approach. However, the stress-strain law of the micromorphic formulation is different, due to the second term on the right-hand side of (28).

## 4. Implementation of implicit gradient model

The implicit gradient formulation, including its distance-based and stress-based modifications, has been implemented into OOFEM (Patzák and Bittnar, 2001; Patzák, 2012), an open-source object-oriented finite element platform available under the GNU license. The implementation is based on mixed finite elements. We start from the strong form of the set of governing differential equations

$$\nabla \cdot \boldsymbol{\sigma} = \mathbf{0} \tag{32}$$

$$\bar{\varepsilon} - \nabla \cdot \left( \boldsymbol{L}^2 \cdot \nabla \bar{\varepsilon} \right) = \tilde{\varepsilon} \tag{33}$$

After multiplication by suitable test functions $\boldsymbol{\xi}$ and $\phi$, integration over $V$ and application of the Gauss theorem, eploiting boundary conditions (21) and (31) with $\boldsymbol{C}$ replaced by $\boldsymbol{L}^2$, equations (32)–(33) are converted to the weak form

$$\int_V \boldsymbol{\sigma} : \nabla_s \boldsymbol{\xi} \, \mathrm{d}V = \int_{S_t} \boldsymbol{t} \cdot \boldsymbol{\xi} \, \mathrm{d}S \tag{34}$$

$$\int_V \left( \bar{\varepsilon}\phi + \nabla \bar{\varepsilon} \cdot \boldsymbol{L}^2 \cdot \nabla \phi - \tilde{\varepsilon}\phi \right) \, \mathrm{dV} = 0 \tag{35}$$

The displacements and the nonlocal equivalent strain are approximated at the element level by

$$\boldsymbol{u} = \boldsymbol{N}\boldsymbol{d} \qquad \bar{\varepsilon} = \boldsymbol{N}_{\bar{\varepsilon}} \boldsymbol{d}_{\bar{\varepsilon}} \tag{36}$$

where $\boldsymbol{N}$ and $\boldsymbol{N}_{\bar{\varepsilon}}$ are matrices containing the shape functions and $\boldsymbol{d}$ and $\boldsymbol{d}_{\bar{\varepsilon}}$ are vectors with the corresponding degrees of freedom (nodal displacements and nodal values of the nonlocal equivalent strain). After conversion of (34)–(35) to the engineering (matrix) notation and discretization based on approximations (36) and on analogous approximations of the test functions, we obtain the set of nonlinear algebraic equations

$$\boldsymbol{f}_{int}(\boldsymbol{d}, \boldsymbol{d}_{\bar{\varepsilon}}) = \boldsymbol{f}_{ext} \tag{37}$$

$$\boldsymbol{\phi}_{int}(\boldsymbol{d}, \boldsymbol{d}_{\bar{\varepsilon}}) = \mathbf{0} \tag{38}$$

in which

$$\boldsymbol{f}_{int} = \int_V \boldsymbol{B}^T \boldsymbol{\sigma} \, \mathrm{d}V \tag{39}$$

and

$$\boldsymbol{f}_{ext} = \int_{S_t} \boldsymbol{N}^T \boldsymbol{t} \, \mathrm{d}S \tag{40}$$

are the standard internal and external forces, and

$$\boldsymbol{\phi}_{int} = \int_V (\boldsymbol{N}_{\bar{\varepsilon}}^T \boldsymbol{N}_{\bar{\varepsilon}} \boldsymbol{d}_{\bar{\varepsilon}} + \boldsymbol{B}_{\bar{\varepsilon}}^T \boldsymbol{L}^2 \boldsymbol{B}_{\bar{\varepsilon}} \boldsymbol{d}_{\bar{\varepsilon}} - \tilde{\varepsilon} \boldsymbol{N}_{\bar{\varepsilon}}^T) \, \mathrm{d}V \tag{41}$$

are the enhanced internal forces. In the equations above, $\boldsymbol{B}$ and $\boldsymbol{B}_{\bar{\varepsilon}}$ are matrices containing derivatives of the shape functions.

The set of nonlinear equations (37)–(38) is solved by the Newton-Raphson iteration scheme. This numerical method requires a tangent matrix, which is obtained by differentiation of the

generalized internal force vector with respect to the nodal unknowns:

$$\boldsymbol{K} = \begin{bmatrix} \dfrac{\partial \boldsymbol{f}_{int}}{\partial \boldsymbol{d}} & \dfrac{\partial \boldsymbol{f}_{int}}{\partial \boldsymbol{d}_{\bar{\varepsilon}}} \\ \dfrac{\partial \boldsymbol{\phi}_{int}}{\partial \boldsymbol{d}} & \dfrac{\partial \boldsymbol{\phi}_{int}}{\partial \boldsymbol{d}_{\bar{\varepsilon}}} \end{bmatrix} \tag{42}$$

For the standard and distance-based approaches, individual blocks of the generalized stiffness matrix are given by

$$\begin{aligned} \frac{\partial \boldsymbol{f}_{int}}{\partial \boldsymbol{d}} &= \int_V (1-\omega)\boldsymbol{B}^T \boldsymbol{D}_e \boldsymbol{B}\, \mathrm{d}V & \frac{\partial \boldsymbol{f}_{int}}{\partial \boldsymbol{d}_{\bar{\varepsilon}}} &= -\int_V \frac{\mathrm{d}g}{\mathrm{d}\bar{\kappa}} \frac{\mathrm{d}\bar{\kappa}}{\mathrm{d}\tilde{\varepsilon}} \boldsymbol{B}^T \bar{\boldsymbol{\sigma}} \boldsymbol{N}_{\bar{\varepsilon}}\, \mathrm{d}V \\ \frac{\partial \boldsymbol{\phi}_{int}}{\partial \boldsymbol{d}} &= -\int_V \boldsymbol{N}_{\bar{\varepsilon}}^T \frac{\partial \tilde{\varepsilon}}{\partial \boldsymbol{\varepsilon}} \boldsymbol{B}\, \mathrm{d}V & \frac{\partial \boldsymbol{\phi}_{int}}{\partial \boldsymbol{d}_{\bar{\varepsilon}}} &= \int_V \left( \boldsymbol{N}_{\bar{\varepsilon}}^T \boldsymbol{N}_{\bar{\varepsilon}} + l^2 \boldsymbol{B}_{\bar{\varepsilon}}^T \boldsymbol{B}_{\bar{\varepsilon}} \right) \mathrm{d}V \end{aligned} \tag{43}$$

For the stress-based approach, the internal length matrix $\boldsymbol{L}^2$ depends on the effective stress state and varies during the simulation. In the derivation of the generalized stiffness, the derivatives of $\boldsymbol{L}^2$ with respect to the displacement degrees of the freedom have to be taken into account. This is easier to handle in subscript notation. The derivative of the $i$-th component of $\phi_{int}$ with respect to the $j$-th component of $\boldsymbol{d}$ is given by

$$\frac{\partial (\phi_{int})_i}{\partial d_j} = \int_V \sum_{n,m} B_{ni}^{\bar{\varepsilon}} \frac{\partial L_{nm}^2}{\partial d_j} G_m^{\bar{\varepsilon}} \mathrm{d}V - \int_V \sum_k N_i^{\bar{\varepsilon}} \frac{\partial \tilde{\varepsilon}}{\partial \varepsilon_k} B_{kj} \mathrm{d}V \tag{44}$$

where $G_m^{\bar{\varepsilon}} = \sum_p B_{mp}^{\bar{\varepsilon}} d_p^{\bar{\varepsilon}}$. The sums are written explicitly because the summation subscripts do not refer to tensorial components but to the components of matrices. For instance, $\varepsilon_k$ is the $k$-th component of the column matrix of engineering strains, which (under plane stress) contains two normal strains and one shear strain (with the meaning of the shear angle). To compute the derivatives of the internal length tensor $\boldsymbol{L}^2$, we exploit its spectral form

$$\boldsymbol{L}^2 = l_1^2 \boldsymbol{n}_1 \otimes \boldsymbol{n}_1 + l_2^2 \boldsymbol{n}_2 \otimes \boldsymbol{n}_2 \tag{45}$$

where $l_1 = l_0$ is constant and $l_2 = \gamma_s l_0$ depends on the effective principal stresses $\hat{\sigma}_1$ and $\hat{\sigma}_2$. Equation (45) can thus be rewritten as

$$\begin{aligned} \boldsymbol{L}^2 &= l_0^2 \boldsymbol{n}_1 \otimes \boldsymbol{n}_1 + \gamma_s^2 l_0^2 \boldsymbol{n}_2 \otimes \boldsymbol{n}_2 = l_0^2 \left( \boldsymbol{I} - \boldsymbol{n}_2 \otimes \boldsymbol{n}_2 \right) + \gamma_s^2 l_0^2 \boldsymbol{n}_2 \otimes \boldsymbol{n}_2 \\ &= l_0^2 \left[ \boldsymbol{I} + \left( \gamma_s^2 - 1 \right) \boldsymbol{n}_2 \otimes \boldsymbol{n}_2 \right] \end{aligned} \tag{46}$$

Recall that $\boldsymbol{n}_1$ and $\boldsymbol{n}_2$ are the unit eigenvectors of the stress tensor (which, for the present isotropic damage model, coincide with the eigenvectors of the strain tensor). Based on the chain rule, the derivative of $L_{nm}^2$ with respect to $d_j$ is computed as

$$\frac{\partial L_{nm}^2}{\partial d_j} = \sum_{k,q} \frac{\partial L_{nm}^2}{\partial \sigma_k} \frac{\partial \sigma_k}{\partial \varepsilon_q} \frac{\partial \varepsilon_q}{\partial d_j} \tag{47}$$

where

$$\frac{\partial \sigma_k}{\partial \varepsilon_q} = (1-\omega) D_{kq}^e \tag{48}$$

and

$$\frac{\partial \varepsilon_q}{\partial d_j} = B_{qj} \tag{49}$$

are components of the material secant stiffness matrix $\boldsymbol{D}_s = (1-\omega)\boldsymbol{D}_e$ and of the strain-displacement matrix $\boldsymbol{B}$, and

$$\begin{aligned}\frac{\partial L_{nm}^2}{\partial \sigma_k} = 2\gamma_s l_0^2 \left( \frac{\partial \gamma_s}{\partial \hat{\sigma}_1}\frac{\partial \hat{\sigma}_1}{\partial \sigma_k} + \frac{\partial \gamma_s}{\partial \hat{\sigma}_2}\frac{\partial \hat{\sigma}_2}{\partial \sigma_k} \right) n_{2n} n_{2m} + \\ + l_0^2(\gamma_s^2 - 1)\left( \frac{\partial n_{2n}}{\partial \sigma_k} n_{2m} + \frac{n_{2n}\partial n_{2m}}{\partial \sigma_k} \right)\end{aligned} \tag{50}$$

The derivatives of $\gamma_s$ with respect to the principal stresses easily follow from (14):

$$\frac{\partial \gamma_s}{\partial \hat{\sigma}_1} = \begin{cases} 2(\beta-1)\dfrac{\hat{\sigma}_2^2}{\hat{\sigma}_1^3} & \text{if } \hat{\sigma}_1 > 0 \text{ and } \hat{\sigma}_2 > 0 \\ \\ 0 & \text{otherwise} \end{cases} \tag{51}$$

$$\frac{\partial \gamma_s}{\partial \hat{\sigma}_2} = \begin{cases} 2(1-\beta)\dfrac{\hat{\sigma}_2}{\hat{\sigma}_1^2} & \text{if } \hat{\sigma}_1 > 0 \text{ and } \hat{\sigma}_2 > 0 \\ \\ 0 & \text{otherwise} \end{cases} \tag{52}$$

In tensorial notation, the derivatives of the principal stresses with respect to the stress tensor are $\partial\hat{\sigma}_1/\partial\boldsymbol{\sigma} = \boldsymbol{n}_1 \otimes \boldsymbol{n}_1$ and $\partial\hat{\sigma}_2/\partial\boldsymbol{\sigma} = \boldsymbol{n}_2 \otimes \boldsymbol{n}_2$. In the engineering notation, this can be rewritten as

$$\frac{\partial \hat{\sigma}_1}{\partial \sigma_k} = N_k^{11} \tag{53}$$

$$\frac{\partial \hat{\sigma}_2}{\partial \sigma_k} = N_k^{22} \tag{54}$$

where

$$N_k^{ij} = \begin{cases} n_{i1}n_{j1} & \text{if } k = 1 \\ n_{i2}n_{j2} & \text{if } k = 2 \\ n_{i1}n_{j2} & \text{if } k = 3 \end{cases} \tag{55}$$

The formula for the derivative of an eigenvector with respect to the tensor can be found e.g. in Šilhavý (1997):

$$\frac{\partial n_{2n}}{\partial \sigma_k} = \frac{n_{1n}\left(N_k^{12} + N_k^{21}\right)}{2(\hat{\sigma}_2 - \hat{\sigma}_1)} \tag{56}$$

Combining equations (47)–(56), we can express the first integrand in (44) as

$$\sum_{n,m} B_{ni}^{\bar{\varepsilon}} \frac{\partial L_{nm}^2}{\partial d_j} G_m^{\bar{\varepsilon}} = \sum_{n,k,m,q} (1-\omega) B_{ni}^{\bar{\varepsilon}} \left[ P_k^1 M_{nm}^{22} + P_k^2 \left( M_{nm}^{12} + M_{nm}^{21} \right) \right] D_{kq}^e B_{qj} G_m^{\bar{\varepsilon}} \tag{57}$$

and the complete expression in (44) can then be rewritten in the compact matrix form as

$$\frac{\partial \boldsymbol{\phi}_{int}}{\partial \boldsymbol{d}} = \int_V \left[ \boldsymbol{B}_{\bar{\varepsilon}}^T \boldsymbol{M}^{22} \boldsymbol{G}_{\bar{\varepsilon}} \boldsymbol{P}^1 \boldsymbol{D}_s \boldsymbol{B} + \boldsymbol{B}_{\bar{\varepsilon}}^T \left( \boldsymbol{M}^{12} + \boldsymbol{M}^{21} \right) \boldsymbol{G}_{\bar{\varepsilon}} \boldsymbol{P}^2 \boldsymbol{D}_s \boldsymbol{B} - \boldsymbol{N}_{\bar{\varepsilon}}^T \frac{\partial \tilde{\varepsilon}}{\partial \boldsymbol{\varepsilon}} \boldsymbol{B} \right] \mathrm{d}V \tag{58}$$

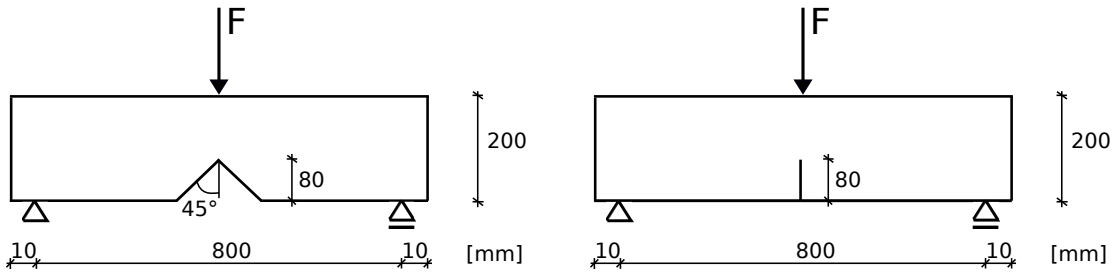


Figure 1: Beam geometry and loading

where

$$\boldsymbol{M}^{ij} = \boldsymbol{n}_i \boldsymbol{n}_j^T \tag{59}$$

$$P_k^1 = 2\gamma_s l_0^2 \left( \frac{\partial \gamma_s}{\partial \hat{\sigma}_1} N_k^{11} + \frac{\partial \gamma_s}{\partial \hat{\sigma}_2} N_k^{22} \right) \tag{60}$$

$$P_k^2 = \frac{l_0^2(\gamma_s^2 - 1)}{2(\hat{\sigma}_2 - \hat{\sigma}_1)} \left( N_k^{12} + N_k^{21} \right) \tag{61}$$

## 5. Numerical examples

In this section we illustrate the implicit gradient formulation and its two modifications by examples of a three-point bending test of a V-notched specimen and of a specimen with an initial crack (sharp notch); see Figure 1 for problem setting. The results are compared to those obtained with a lattice model; see Grassl and Jirásek (2010) for the description of the lattice model and Xenos et al. (2013) for comparison of the lattice model with an integral nonlocal damage model.

In the present simulations, the equivalent strain is defined by the expression

$$\tilde{\varepsilon} = \frac{1}{E} \max_I \bar{\sigma}_I \tag{62}$$

based on the Rankine condition of maximum principal stress. The damage law is taken according to Grassl and Jirásek (2010) as

$$g(\kappa) = \begin{cases} 1 - \exp\left( -\dfrac{1}{m_d} \left( \dfrac{m_d}{\varepsilon_{max}} \right)^{m_d} \right) \\ \\ 1 - \dfrac{\varepsilon_3}{\kappa} \exp\left( \dfrac{\kappa - \varepsilon_1}{\varepsilon_f \left[ 1 + \frac{\kappa - \varepsilon_1}{\varepsilon_2} \right]^n} \right) \end{cases} \tag{63}$$

The independent model parameters are $E$ = Young's modulus, $\nu$ = Poisson's ratio, $f_t$ = uniaxial tensile strength, $\varepsilon_{max}$ = strain at the peak of the uniaxial tensile stress-strain curve, and parameters $\varepsilon_1$, $\varepsilon_2$ and $n$ affecting the shape of the softening part of the curve. The dependent

| Elastic parameters | |
|---|---|
| $E$ | 29.6 GPa |
| $\nu$ | 0.2 |
| Parameters of damage law | |
| $f_t$ | 2.86 MPa |
| $\varepsilon_{max}$ | 0.000198 |
| $\varepsilon_1$ | 0.00023 |
| $\varepsilon_2$ | 0.007 |
| $n$ | 0.85 |
| Nonlocal parameters | |
| $l$ | 4 mm |
| $t$ | 1 |
| $\beta$ | 0.35 |

Table 1: Material parameters

parameters are evaluated as

$$m_d = \frac{1}{\ln\left(E\varepsilon_{max}/f_t\right)} \tag{64}$$

$$\varepsilon_f = \frac{\varepsilon_1}{\left(\varepsilon_1/\varepsilon_{max}\right)^{m_d} - 1} \tag{65}$$

$$\varepsilon_3 = \varepsilon_1 \exp\left(-\frac{1}{m_d}\left(\frac{\varepsilon_1}{\varepsilon_{max}}\right)^{m_d}\right) \tag{66}$$

The values of material parameters have been taken from Xenos et al. (2013) and are summarized in Tab. 1. In Grassl and Jirásek (2010), these parameters were calibrated by fitting the results of simulations of the uniaxial tensile test using a meso-scale model. The same meso-scale model was used by Xenos et al. (2013) in simulations of the bending test, which did not lead to any excessive dissipation near the tip of a notch.

The present results are shown in the form of the load-displacement curves (Fig. 2) and cumulated dissipated energy along the height of the beam (Figs. 3 and 4). The peak load and dissipated energy of the meso-scale model are overestimated by the standard and also by the modified models for both beam geometries. The distance-based formulation leads to a somewhat better agreement with the meso-scale model. The stress-based model provides slightly better results for the beam with a sharp crack, while for the V-notched specimen the results remain surprisingly close to the standard approach.

## 6. Conclusion

In this paper, a gradient-enhanced damage model and its two modifications have been described and applied to the modelling of a three-point bending test with different geometries. For the beam with a sharp notch, the distance-based and stress-based formulations reduce the dissipated energy near the notch and the results are in a better agreement with the meso-scale model. For the V-notched specimen the distance-based model is in a better agreement with the meso-scale

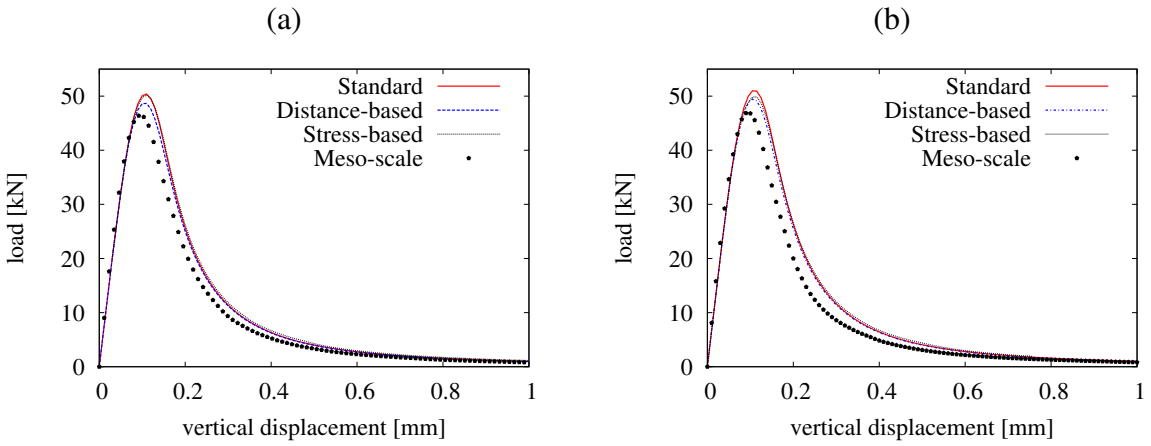


Figure 2: Load-displacement curve: (a) V-notch, (b) sharp notch

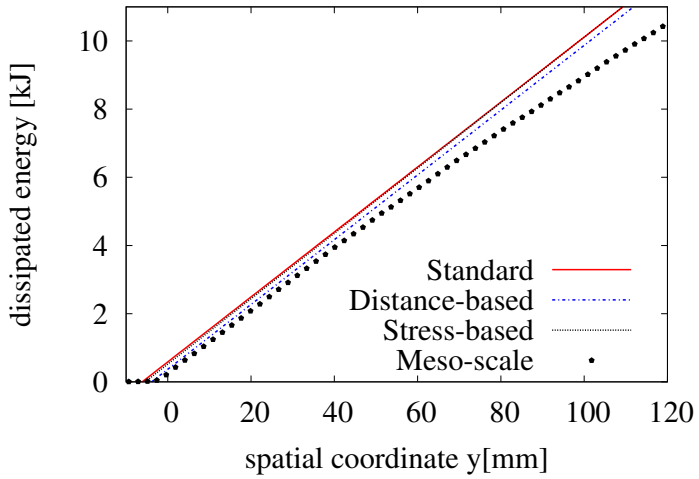


Figure 3: Dissipated energy: V-notched specimen

approach while the stress-based model provides no improvement as compared to the standard formulation.

Further research will focus on the comparison of the computational efficiency of the presented modifications with the integral approach, on the influence of different equivalent strain measures on the load-displacement curve and on the dissipated energy, and on the links between the implicit gradient formulation and the thermodynamically consistent micromorphic model. Furthermore, the distance-based and stress-based modification will be used with a damage-plasticity model, which is more suitable for a realistic description of concrete failure in complex situations.

## 7. Acknowledgment

Financial support received from the Czech Technical University in Prague under grant SGS13/034/OHK1/1T/11 is gratefully acknowledged.

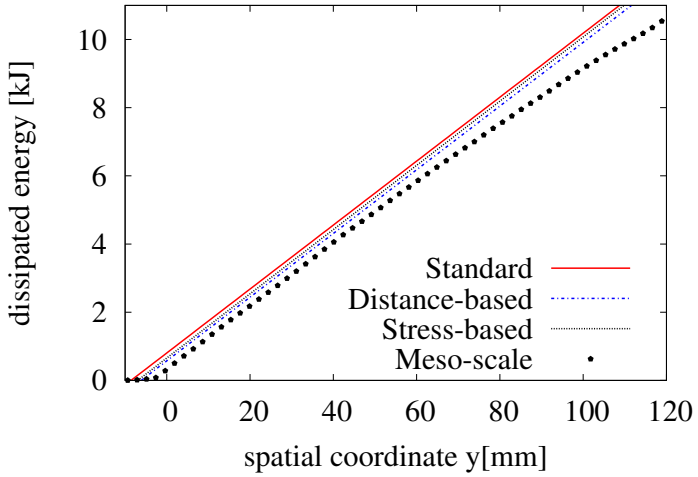


Figure 4: Dissipated energy: specimen with a sharp notch

## 8. References

Bažant, Z. P., Le, J.-L. & Hoover, C. G. 2010: Nonlocal boundary layer (nbl) model: overcoming boundary condition problems in strength statistics and fracture analysis of quasibrittle materials. *Fracture Mechanics of Concrete and Concrete Structures*, 135–143

Forest, S. 2009: Micromorphic approach for gradient elasticity, viscoplasticity, and damage. *Journal of Engineering Mechanics*, Vol. 135, 117–131

Giry, C., Dufour, F. & Mazars, J. 2011: Stress-based nonlocal damage model. *International Journal of Solids and Structures*, Vol.48, 34313443

Grassl, P. & Jirásek, M. 2010: Meso-scale approach to modelling the fracture process zone of concrete subjected to uniaxial tension. *International Journal of Solids and Structures*, Vol. 47, 957–968

Xenos, D., Grassl, P. & Jirásek M. 2013: Evaluation of nonlocal approaches for modelling fracture in notched concrete specimens. *Fracture Mechanics of Concrete and Concrete Structures*

Jirásek, M., Rolshoven, S. & Grassl, P. 2004: Size effect on fracture energy induced by nonlocality. *International Journal of Numerical and Analytical Methods in Geomechanics*, Vol. 28, 653–670

Patzák, B. & Bittnar, Z. 2001: Design of object oriented finite element code. *Advances in Engineering Software*, Vol. 32, 759–767

Patzák, B. 2012: OOFEM – an object-oriented simulation tool for advanced modeling of materials and structures. *Acta Polytechnica*, Vol. 52, 59–66

Šilhavý, M. 1997: Mechanics and thermomechanics of continuous media. Springer, Berlin.